MNRAS **436,** 2892–2906 (2013)
Advance Access publication 2013 October 28
doi:10.1093/mnras/stt1548

The cosmic evolution of the IMF under the Jeans conjecture with implications for massive galaxies

Desika Narayanan[1,2★,†] and Romeel Davé[2,3,4,5]

[1]*Department of Astronomy, Haverford College, 370 Lancaster Ave, Haverford, PA 19041, USA*
[2]*Steward Observatory, University of Arizona, 933 N Cherry Ave, Tucson, AZ 85721, USA*
[3]*University of the Western Cape, 7535 Bellville, Cape Town, South Africa*
[4]*South African Astronomical Observatories, Observatory, Cape Town, 7925, South Africa*
[5]*African Institute for Mathematical Sciences, Muizenberg, Cape Town, 7945, South Africa*

Accepted 2013 August 15. Received 2013 August 14; in original form 2012 October 21

ABSTRACT

We examine the cosmic evolution of a stellar initial mass function (IMF) in galaxies that varies with the Jeans mass in the interstellar medium, paying particular attention to the *K*-band stellar mass-to-light ratio (M/L_K) of present-epoch massive galaxies. We calculate the typical Jeans mass using high-resolution hydrodynamic simulations coupled with a fully radiative model for the interstellar medium (ISM), which yields a parametrization of the IMF characteristic mass as a function of galaxy star formation rate (SFR). We then calculate the star formation histories of galaxies utilizing an equilibrium galaxy growth model coupled with constraints on the star formation histories set by abundance matching models. We find that at early times, energetic coupling between dust and gas drives warm conditions in the ISM, yielding bottom-light/top-heavy IMFs associated with large ISM Jeans masses for massive star-forming galaxies. Owing to the remnants of massive stars that formed during the top-heavy phases at early times, the resultant $M/L_K(\sigma)$ in massive galaxies at the present epoch is *increased* relative to the non-varying IMF case. At late times, lower cosmic ray fluxes allow for cooler ISM temperatures in massive galaxies, and hence newly formed clusters will exhibit bottom-heavy IMFs, further increasing $M/L_K(\sigma)$. Our central result is hence that a given massive galaxy may go through both top-heavy and bottom-heavy IMF phases during its lifetime, though the bulk of the stars form during a top-heavy phase. Qualitatively, the variations in $M/L_K(\sigma)$ with galaxy mass are in agreement with observations; however, our model may not be able to account for bottom-heavy mass functions as indicated by stellar absorption features.

Key words: stars: formation – stars: luminosity function, mass function – galaxies: formation – galaxies: high-redshift – galaxies: ISM – galaxies: starburst – cosmology: theory.

1 INTRODUCTION

The stellar initial mass function (IMF) is fundamental for understanding a wide range of problems in astrophysics. The IMF provides a mechanism for parametrizing the distribution of masses of stars formed in a given generation. Beyond being a crucial ingredient for any successful theory of star formation (e.g. McKee & Ostriker 2007), the IMF determines such galactic properties as the metal enrichment history, energy distribution of photons injected into the interstellar medium (ISM), and conversion of luminosities into physical quantities such as star formation rates (SFRs) and stellar masses (M_*).

Despite the obvious importance of the IMF, no consensus exists that describes its origin and possible variations. In the Milky Way, direct star counts have found that the IMF may be well parametrized by a single power law (Salpeter 1955), a multi-segment power law (e.g. Kroupa, Tout & Gilmore 1993; Kroupa 2002, hereafter, 'Kroupa-like' IMFs), or a lognormal (e.g. Miller & Scalo 1979; Chabrier 2003). Generally, observations have found at most mild variations in the IMF within the Galaxy (Bastian, Covey & Meyer 2010).

From a theoretical standpoint, a broad range of models for the origin of the IMF exist. The central ideas behind these range from giant molecular cloud (GMC) Jeans mass arguments (Larson 1998, 2005; Bate & Bonnell 2005; Tumlinson 2007; Elmegreen, Klessen & Wilson 2008; Narayanan & Davé 2012) to protostellar feedback models (Silk 1995; Adams & Fatuzzo 1996; Bate 2009; Krumholz 2011) to models of a turbulent ISM (Padoan & Nordlund 2002;

★ E-mail: dnarayanan@as.arizona.edu
† Bart J Bok Fellow.

Hennebelle & Chabrier 2008; Hopkins 2012). While the driving physics behind the origin of the IMF varies substantially, nearly all theories suggest that the IMF should vary with changing physical conditions, even if relatively weakly (cf. Elmegreen et al. 2008; Krumholz 2011). Though there is currently no unambiguous direct evidence for systematic variations of the IMF with environmental conditions (Bastian et al. 2010), the last decade of observations have provided tantalizing *indirect* evidence for two emerging trends in IMF variations.

The first suggests that the IMF may be bottom-heavy (defined as an excess of the ratio of low-mass stars to high-mass stars with respect to a Milky Way IMF) in present-epoch early-type galaxies. Complementary observational techniques have arrived at this conclusion, adding to its robustness. For example, recent observations of gravity-sensitive stellar absorption lines (such as FeH – the 'Wing-Ford' band – Ca II, and Na I among others) combined with new empirical stellar libraries of cool stars (Rayner, Cushing & Vacca 2009) have been able to distinguish K and M dwarfs from K and M giants, and found the IMF to be bottom-heavy in $z \sim 0$ early-type galaxies (Wing & Ford 1969; van Dokkum & Conroy 2010, 2012; Conroy & van Dokkum 2012a,b; Ferreras et al. 2012; Spiniello et al. 2012; Smith, Lucey & Carter 2012). Meanwhile, observed constraints on the stellar mass-to-light (M/L) ratio from stellar kinematics have arrived at the same conclusion (e.g. Auger et al. 2010; Treu et al. 2010; Spiniello et al. 2011; Brewer et al. 2012; Cappellari et al. 2012a,b; Dutton et al. 2012; Tortora, Romanowsky & Napolitano 2012). Interestingly, both methods find that the IMF varies systematically in a manner that more massive galaxies have increasingly bottom-heavy IMFs.

If elliptical galaxies are the end-product of massive starbursts, then the implication is that the IMF may show an excess of low-mass stars in heavily star-forming environments. This is, however, in direct contrast to a number of indirect measurements of the IMF in starbursts which all argue that the IMF may be *top-heavy* in these environments, rather than bottom-heavy. Evidence for this second trend in IMF variations comes from a variety of complementary albeit indirect measurements.

Tacconi et al. (2008) performed simultaneous modelling of the stellar masses, CO–H_2 conversion factors and stellar IMFs of $z \sim 2$ Submillimetre-selected galaxies (SMGs), the most rapidly star-forming galaxies in the Universe, and found a best-fitting model with a M/L ratio roughly half that of a standard Kroupa IMF. Similarly, van Dokkum (2008) suggested that the colour evolution and M/L ratios for $z \sim 1$ early-type galaxies may best be explained by a bottom-light IMF. More indirect evidence comes from models that have appealed to a top-heavy IMF at $z \sim 2$ to resolve the noted discrepancy between the observed SFR–M_* relation and simulated one (Davé 2008).

Some evidence for a top-heavy IMF in heavily star-forming systems at $z \sim 0$ exists as well. For example, Rieke et al. (1993) and Förster Schreiber et al. (2003) suggest that the IMF may have a turnover mass a factor of ∼2–6 larger than traditional Kroupa (2002) IMF in the nearby starburst galaxy M82 (though see Satyapal et al. 1997). Similarly, a simultaneous fit to the present-day K-band luminosity density, observed cosmic SFR density and cosmic background radiation by Fardal et al. (2007) suggest a 'paunchy' IMF wherein there is an excess of intermediate-mass stars. Utilizing a sample of ∼33 000 galaxies, Gunawardhana et al. (2011) find evidence for a strong IMF–SFR relation in galaxies, such that heavily star-forming systems appear to have a more top-heavy IMF. Even in the Galactic Centre, observations suggest that a top-heavy IMF may apply (Nayakshin & Sunyaev 2005; Stolte et al. 2005). While all of these observations can be explained without the need for IMF variations,[1] it is compelling that when a variable IMF is inferred for a high-SFR surface density environment, it invariably tends towards top-heavy.

In short, while the evidence is by no means firm, deviations from a Milky Way IMF appear to follow two trends: in present-day ellipticals, the IMF tends towards an excess of low-mass stars, whereas in heavily star-forming galaxies from $z \sim 0$–2, the IMF appears to have an excess of high-mass stars. Simultaneously understanding the origin of both of these trends presents a challenge for any theory of the IMF.

One possibility is that systematic variations in the IMF owe to varying physical conditions in the star-forming molecular ISM. Jeans (1902) and others (e.g. Larson 2005; Bate & Bonnell 2005; Klessen, Spaans & Jappsen 2007; Tumlinson 2007; Narayanan & Davé 2012) have postulated that the characteristic stellar mass formed may relate to the fragmentation properties of the parent molecular cloud (this is commonly known as the 'Jeans conjecture'). In this picture, the temperature and density of the molecular cloud ($M_J \sim T^{3/2}/n^{1/2}$) determine the minimum fragmentation mass of the cloud, and thus set the stellar mass scale.

In this paper, we explore the cosmic evolution of the IMF in galaxies under the Jeans conjecture to examine whether a stellar IMF that varies with the Jeans masses of molecular clouds can explain the tentative evidence for bottom-heavy IMFs in early-type galaxies as well as the purported top-heavy IMF in high-SFR density galaxies. It is important to note that we neither argue for or against the aforementioned observed IMF trends, but rather take them as a given. Similarly, we make no claims regarding the validity of the Jeans conjecture, but rather seek to assess its plausibility by examining the cosmological consequences of a stellar IMF that varies with the Jeans mass in molecular clouds. In Section 2, we describe our methods, detailing our galaxy formation models as well as model for the molecular ISM. In Section 3, we report our main results, and in Section 4, we provide discussion. Finally, in Section 5, we summarize.

2 GALAXY EVOLUTION AND ISM MODELS

2.1 Summary of methods

Our principal goal in this work is to model the cosmic evolution of the IMF under the assumption that the IMF varies with the Jeans properties of molecular clouds. Because resolving molecular cloud scales (∼10 s of pc) in cosmological volumes is intractable for all but a few galaxies (e.g. Christensen et al. 2012), we have developed a multi-scale methodology in order to model the mean ISM properties for an ensemble of galaxies.

Our first goal is to parametrize the mean molecular ISM physical properties in terms of a global property. To do this, we employ a large suite of relatively high-resolution smoothed particle hydrodynamic (SPH) simulations of isolated disc galaxies and galaxy mergers in evolution. These galaxies sample a range of galaxy masses and merger mass ratios, with the main goal being to simulate a large dynamic range of physical conditions. These models can marginally resolve the surfaces of the most massive GMCs (∼70 pc), and employ a fully radiative sub-resolution model for the physical and chemical state of GMCs below the resolution limit. We consider

[1] In Section 4, we review many of the arguments against a varying IMF in the context of the aforementioned examples.

the main physical processes that determine the thermal structure of the GMCs, and thus are able to resolve their Jeans properties. As we will show, the high-resolution SPH galaxy evolution simulations show that the average Jeans mass in a molecular cloud scales well with the galaxy's SFR.

We then aim to understand the cosmic evolution of the Jeans properties of GMCs, and hence the stellar IMF. We model the cosmic evolution of the physical properties of galaxies utilizing the analytic methodology described in Davé, Finlator & Oppenheimer (2012). This methodology describes the evolution of the galaxy SFR, stellar mass growth and metal enrichment while assuming that galaxies live in an equilibrium between gas inflows, outflows and consumption via star formation. The results of the analytic models provide a good match to the evolution of the physical properties of bona fide hydrodynamic cosmological simulations, but at a substantially reduced computational cost. The main output from these models is the star formation histories for galaxies of various masses. Combined with a model for how the average Jeans properties of molecular clouds vary with the galaxy-wide SFR (as informed from the high-resolution hydrodynamic galaxy evolution simulations), these models then describe the cosmic evolution of the IMF under the Jeans conjecture.

Finally, we combine these results with population synthesis models (FSPS; Conroy, Gunn & White 2009; Conroy, White & Gunn 2010; Conroy & Gunn 2010) in order to explore the observable properties of stellar populations under a varying IMF. We utilize these to compare directly against observations.

2.2 Hydrodynamic Galaxy evolution models

We simulate the hydrodynamic evolution of a large library of idealized isolated disc galaxies and galaxy mergers using a modified version of the publicly available code GADGET-2[2] (Springel & Hernquist 2003; Springel, Di Matteo & Hernquist 2005; Springel 2005). The galaxies range in baryonic mass from $\sim 10^{10}\,\mathrm{M}_{\odot}$ to $\sim 10^{12}\,\mathrm{M}_{\odot}$, and their physical properties are listed in full in table A1 of Narayanan et al. (2012a). We simulate mergers between these discs with mass ratio 1:10, 1:3 and 1:1. Similarly, the initial orbital configurations are given in Narayanan et al. (2012a).

The disc galaxies are exponential and initialized according to the Mo, Mao & White (1998) model. They are embedded in a live dark matter halo with a Hernquist (1990) density profile. Mergers simply involve two discs initialized as such. The halo concentration and virial radius of the galaxies are motivated by cosmological *N*-body simulations, and are redshift dependent (Bullock et al. 2001; Robertson et al. 2006). We simulate galaxies scaled for $z = 0$ and $z = 3$. The gravitational softening lengths are $\sim 100\,h^{-1}$ pc for baryons, and $\sim 200\,h^{-1}$ pc for dark matter.

The $z = 0$ galaxies are initialized with a 40 per cent baryonic gas fraction, and $z = 3$ galaxies with an 80 per cent baryonic gas fraction. These gas fractions are potentially larger than those observed (e.g. Daddi et al. 2010; Tacconi et al. 2010; Narayanan, Bothwell & Davé 2012b). However, because we do not include any form of gas replenishment from the intergalactic medium (IGM) in these idealized simulations (e.g. Moster et al. 2011, 2012), we require large initial gas fractions in order to have substantial lifetimes of moderately gas-rich galaxies during the evolution of the merger. When galaxies merge, this is necessary to drive a starburst (Narayanan et al. 2010a; Hayward et al. 2011, 2012a). In any case, the exact choice of initial gas fraction is not terribly relevant as we principally simulate the evolution of idealized galaxies in order to build a sample of galaxies with a large dynamic range of physical conditions. The gas is initialized as primordial. A mass fraction of stars (utilizing a Salpeter IMF) are assumed to die instantly upon each star formation event, and enrich the surrounding ISM with metals assuming instantaneous recycling and a yield of 0.02 (Springel & Hernquist 2003).

Within the hydrodynamic evolution of the galaxies, the ISM is modelled as multi-phase, with cold, star-forming clouds embedded in a hotter, pressure-confining phase (McKee & Ostriker 1977; Springel & Hernquist 2003). These phases can exchange mass via supernova heating of cold clouds and radiative cooling of the hotter phase. Stars form according to a volumetric Schmidt (1959) power-law relation with index 1.5 (Kennicutt 1998a). The normalization is set to match the local surface density Σ_{SFR}–Σ_{gas} relation (Kennicutt 1998b). We note that while both the slope and normalization of the Kennicutt–Schmidt star formation law are the subject of heavy debate (see e.g. Krumholz & Thompson 2007; Bigiel et al. 2008; Narayanan, Cox & Hernquist 2008a; Narayanan et al. 2008b; Ostriker, McKee & Leroy 2010; Ostriker & Shetty 2011; Narayanan et al. 2011a; Kennicutt & Evans 2012; Krumholz, Dekel & McKee 2012; Narayanan & Davé 2012, for just a few examples), we showed in Narayanan et al. (2011b) that the physical conditions in the ISM are relatively insensitive to these parameters so long as power-law indices between $\sim$1 and 2 are adopted.

2.3 Molecular gas ISM specification

We determine the physical and chemical properties of the molecular gas in the SPH galaxy evolution simulations in post-processing. We describe the methodology in full in Narayanan et al. (2011b), though summarize the relevant details here.

2.3.1 Cloud chemical and physical state

We first project the physical properties of the SPH particles on to an adaptive mesh using the SPH smoothing kernel. The base mesh is 5^3 spanning 200 kpc on a side, and recursively refine in an oct-subdivision based on the refinement criteria that the relative density of metals should be less than 0.1, and that the *V*-band optical depth across a cell be less than unity. The smallest cells refined to $\sim$70 pc across, just resolving massive GMCs.

GMCs within the cells are modelled as spherical and isothermal. The H_2 fraction is determined by balancing photodissociation rates by Lyman–Werner band photons against H_2 formation rates on dust grains. For simplicity, we utilize the analytic prescription of Krumholz, McKee & Tumlinson (2008, 2009a,b) which assumes equilibrium chemistry. A comparison of this model against full radiative transfer models suggests that this approximation is reasonable for metallicities above $Z > 0.01\,\mathrm{Z}_{\odot}$, and all our galaxies' metallicities are well above this.

The GMCs are assumed to be of constant density. In order to treat GMCs that reside in large cells in the adaptive mesh (and avoid unphysical conditions), we establish a floor surface density of $100\,\mathrm{M}_{\odot}\ \mathrm{pc}^{-2}$. This value is motivated by observations of Local Group GMCs (Bolatto et al. 2008; Fukui & Kawamura 2010). Generally, in heavily star forming systems, the mass-weighted surface density of GMCs is much larger than this, and the floor value is never reached (Narayanan et al. 2011b). For these 'resolved' GMCs, the

[2] In practice, we use GADGET-3 where the principal modifications employed here involve processor load balancing.

cloud is assumed to occupy the entire cubic volume of the cell that it resides in. In lower SFR systems, however, the bulk of the GMCs have $\Sigma_{\rm H2} \approx 100\,{\rm M}_\odot\ {\rm pc}^{-2}$.

With the H_2 mass and cloud surface density established, and an assumption regarding the GMC geometry (either spherical[cubic] if the cloud is unresolved[resolved]), the density is known. GMCs are known to be supersonically turbulent (McKee & Ostriker 2007, and references therein). We allow for the turbulent compression of gas by scaling the volumetric densities of the GMCs by a factor $e^{\sigma_\rho^2/2}$, where numerical simulations show that for supersonic turbulence:

$$\sigma_\rho^2 \approx \ln\left(1 + 3M_{\rm 1D}^2/4\right) \quad (1)$$

where $M_{\rm 1D}$ is the one-dimensional Mach number (Ostriker, Stone & Gammie 2001; Padoan & Nordlund 2002, though see Lemaster & Stone 2008). As we will show, the temperature calculation of the GMCs is dependent on the densities. Because solving for the density compressions and temperatures simultaneously for many millions of cells across thousands of galaxy snapshot realizations is a computationally prohibitive task, we assume the temperature of the GMC is 10 K for the sound speed calculation.

2.3.2 *Cloud thermal state*

The other pertinent variable for calculating the Jeans properties of the model GMCs is the gas kinetic temperature. Our model is based on that laid out by Goldsmith (2001) and Krumholz, Leroy & McKee (2011). The dominant gas heating terms are by grain photoelectric effect at a rate per H nucleus $\Gamma_{\rm pe}$, cosmic ray heating at a rate $\Gamma_{\rm CR}$, and cooling via either C II fine structure line cooling, or ^{12}CO rotational line cooling at a rate $\Lambda_{\rm line}$. Finally, there is an energy exchange between the dust and gas at a rate $\Psi_{\rm gd}$. We assume thermal balance between the gas and dust which gives the following equations that are solved simultaneously by iterating on the temperatures of the gas and dust:

$$\Gamma_{\rm pe} + \Gamma_{\rm CR} - \Lambda_{\rm line} + \Psi_{\rm gd} = 0 \quad (2)$$

$$\Gamma_{\rm dust} - \Lambda_{\rm dust} - \Psi_{\rm gd} = 0. \quad (3)$$

We assume that the photoelectric heating rate is attenuated by half the mean extinction of the cloud, such that:

$$\Gamma_{\rm pe} = 4 \times 10^{-26} G_0' e^{-N_{\rm H}\sigma_{\rm d}/2}\ {\rm erg\ s^{-1}} \quad (4)$$

where G_0' is the FUV intensity relative to the solar neighbourhood, and $\sigma_{\rm d}$ is the dust cross-section per H atom to UV photons. For simplicity, we assume that the $G_0' = 1$ and $\sigma_{\rm d} = 1 \times 10^{-21}\ {\rm cm}^{-2}$, though we note that tests that involve scaling the Habing field by the SFR make little difference on the thermal properties of our clouds owing to strong shielding (Narayanan et al. 2011b).

The cosmic ray heating rate is given by

$$\Gamma_{\rm CR} = \zeta' q_{\rm CR}\ {\rm s^{-1}} \quad (5)$$

where ζ' is the cosmic ray ionization rate (here, assumed to be $2 \times 10^{-17} Z'\ {\rm s^{-1}}$), and $q_{\rm CR}$ is the thermal energy increase per cosmic ray ionization. For H_2, $q_{\rm CR} \approx 12.25$ eV (though note that this value is quite uncertain; see discussion in appendix A4 of Krumholz et al. 2011), and for H I, $q_{\rm CR} \approx 6.5$ eV (Dalgarno & McCray 1972).

An important aspect of these calculations is that we assume the cosmic ray heating rate scales linearly with the galaxy-wide SFR, anchored by an assumed Milky Way SFR of $2\,{\rm M}_\odot\ {\rm yr}^{-1}$ (Robitaille & Whitney 2010; Chomiuk & Povich 2011). While the exact scaling between the cosmic ray ionization rate and SFR is unknown, some observational evidence exists suggesting a linear relationship. Observations of M82 by the VERITAS group, as well as γ-ray observations[3] of the Galaxy, Large Magellanic Cloud, NGC 253 and M82 by the *FERMI* group all suggest a linear relation between the galaxy-wide SFR and cosmic rays (Acciari et al. 2009; Abdo et al. 2010).

The dust temperature is calculated via full 3D Monte Carlo radiative radiative transfer. We utilize SUNRISE, a publicly available dust radiative transfer simulation package (Jonsson 2006; Jonsson et al. 2006; Jonsson, Groves & Cox 2010; Jonsson & Primack 2010). The detailed algorithms are described in Jonsson et al. (2010), and we only summarize here.

The sources of light are stellar clusters and an AGN which acts in the hydrodynamic simulations as a sink particle that accretes according to a Bondi–Hoyle–Lyttleton parametrization (Bondi & Hoyle 1944). The stars emit a STARBURST99 spectrum (Leitherer et al. 1999; Vázquez & Leitherer 2005), where the ages and metallicities derive from the SPH calculations. The AGN emits a luminosity-dependent SED based on the Hopkins, Richards & Hernquist (2007) templates that derive from observations of unreddened type I quasars. In practice, the AGN does not impact our results significantly (see tests by Narayanan et al. 2011b). The radiation traverses the ISM, and is scattered, absorbed and re-emitted until the dust temperatures converge. The dust and radiation field are assumed to be in radiative equilibrium. The dust mass is set by assuming a constant dust-to-metals ratio of 0.4, comparable to that of the Milky Way (Dwek 1998; Vladilo 1998; Calura, Pipino & Matteucci 2008), and we utilize the Weingartner & Draine (2001) $R = 3.15$ dust grain models with Draine & Li (2007) updates.

For disc galaxies at low redshift, we assume that young (<10 Myr) stellar clusters are embedded in photodissociation regions and H II regions for 2–3 Myr. In this case, the STARBURST99 spectrum is replaced by SEDs derived from MAPPINGSIII photoionization calculations (Groves et al. 2008; Jonsson et al. 2010). The covering time-scale is motivated by parameter-space surveys by Jonsson et al. (2010) who showed that this parameter choice produces synthetic SEDs of $z = 0$ disc galaxies comparable to those observed in the *Spitzer* Infrared Nearby Galaxy Survey (SINGS; Kennicutt et al. 2003).

For galaxy mergers at $z = 0$ and all galaxies at $z = 3$, the stellar densities become so high that stellar clusters overlap. In this case, using MAPPINGSIII no longer makes sense as the super-stellar clusters (sometime as massive as $\sim 10^8\,{\rm M}_\odot$) saturate the MAPPINGSIII photoionization models. In these cases, we assume the cold ISM is a uniform medium with a volume filling factor of unity. Observations of nearby starburst galaxies may support this picture for the cold ISM structure in heavily star-forming galaxies (Downes & Solomon 1998; Sakamoto et al. 1999). Beyond this, in tests run in the appendix of Narayanan et al. (2011b), we found that the thermal and physical properties of the molecular ISM were generally robust against the choices made for the PDR clearing time or ISM volume filling factor.

The line cooling is assumed to happen either via C II or CO. The fraction of hydrogen where carbon is mostly in the form of CO is well approximated by (Wolfire, Hollenbach & McKee 2010; Glover & Mac Low 2011)

$$f_{\rm CO} = f_{\rm H2} \times {\rm e}^{-4(0.53 - 0.045\ \ln\ \frac{G_0'}{n_{\rm H}/{\rm cm^{-3}}} - 0.097\ \ln Z')/A_{\rm v}}. \quad (6)$$

[3] γ-rays can arise as the result of cosmic ray interactions with H_2, via pion-decay.

When this fraction is greater than 0.5, we assume the cooling happens via CO rotational lines; otherwise, the cooling is dominated by C II emission. We assume a constant carbon to H_2 abundance of $1 \times 10^{-4} \times Z'$ (Lee, Bettens & Herbst 1996), where Z' is the metallicity with respect to solar.

To determine the cooling rates, we utilize one-dimensional escape probability calculations (Krumholz & Thompson 2007). The level populations of the molecule are assumed to be in statistical equilibrium, and determined through the rate equations:

$$\sum_l (C_{\rm lu} + \beta_{\rm lu} A_{\rm lu}) f_l = \left[\sum_u (C_{\rm ul} + \beta_{\rm ul} A_{\rm ul}) \right] f_u \tag{7}$$

$$\sum_i f_i = 1 \tag{8}$$

where C are the collisional rates,[4] $A_{\rm ul}$ are the Einstein coefficients for spontaneous emission, f the fractional level populations, and $\beta_{\rm ul}$ is the escape probability for transition $u \rightarrow l$. The rate equations can be rearranged as an eigenvalue problem, and solved accordingly.

The escape probability, $\beta_{\rm ul}$, can be approximately related to the line optical depth $\tau_{\rm ul}$ (Draine 2011) via:

$$\beta_{\rm ul} \approx \frac{1}{1 + 0.5\tau_{\rm ul}} \tag{9}$$

and the optical depth is

$$\tau_{\rm ul} = \frac{g_u}{g_l} \frac{3 A_{\rm ul} \lambda_{\rm ul}^3}{16(2\pi)^{3/2}\sigma} Q N_{\rm H2} f_l \left(1 - \frac{f_u g_l}{f_l g_u}\right) \tag{10}$$

where Q is the abundance of CO with respect to H_2, g_l and g_u are the statistical weights of the levels, $N_{\rm H2}$ is the column density of H_2 through the cloud, $\lambda_{\rm ul}$ is the wavelength of the transition, and σ is the velocity dispersion in the cloud.

The 1D velocity dispersion, σ, is calculated by

$$\sigma = \max(\sigma_{\rm cell}, \sigma_{\rm vir}). \tag{11}$$

Here, $\sigma_{\rm cell}$ is the mean square sum of the subgrid turbulent velocity and the resolved non-thermal velocity dispersion. The turbulent velocity is calculated from the external pressure from the hot ISM (Robertson et al. 2004), though we impose a ceiling of 10 km s^{-1} which is informed by simulations of turbulent energy driving and dissipation (Dib, Bell & Burkert 2006; Joung, Mac Low & Bryan 2009; Ostriker & Shetty 2011). The resolved non-thermal component is calculated as the mean of the standard deviation of the velocities of the nearest neighbour cells in the three cardinal directions. A floor velocity dispersion of $\sigma_{\rm vir}$ is established (typically for poorly resolved GMCs) by assuming the GMC is in virial balance with $\alpha_{\rm vir} = 1$, with $\alpha_{\rm vir} \equiv 5\sigma_{\rm vir}^2 R/(GM)$.

With these elements in place, we then iterate equations (2) and (7)–10 in order to determine the equilibrium gas temperature.

Finally, we note that our model does not include any effects of X-ray heating of gas from either massive stars or accreting compact objects (e.g. Hocuk & Spaans 2010, 2011). This may increase gas heating beyond the contribution of gas–dust coupling, or cosmic rays in rather extreme environments.

[4] The rate coefficients are taken from the *Leiden Atomic and Molecular Database* (Schöier et al. 2005).

2.4 Cosmological models

As will be discussed in Section 3, the temperature (and more generally, the average Jeans mass of a GMC) in a galaxy scales with the galaxy-wide SFR. In order to understand the cosmic evolution of the physical properties of galaxies, and therefore the stellar IMF, we must turn to cosmological galaxy evolution models.

Davé et al. (2012) presented analytic models that describe the cosmic evolution of the stellar, gaseous and metal content of galaxies under the condition that they lie in a slowly evolving (with redshift) equilibrium state between gas infall from the IGM, gas outflows and gas consumption from star formation. These models compare quite well to the results from cosmological hydrodynamic simulations (e.g. Oppenheimer et al. 2010), though have the practical advantage of being computationally inexpensive. We therefore utilize these and summarize the relevant aspects of the model here.

In this model, the SFR is determined by the gas infall rate minus the outflow rate, which is given by the mass loading factor η times the SFR. The gas infall rate is mitigated by a preventive feedback parameter $\zeta < 1$, while it is augmented by recycling of winds governed by the recycling parameter α_Z (Finlator & Davé 2008), which is the ratio of the infalling gas metallicity to the ISM gas-phase metallicity. The SFR is given by

$$\mathrm{SFR} = \frac{\zeta \dot{M}_{\rm grav}}{(1+\eta)(1-\alpha_Z)}. \tag{12}$$

Hence there are three parameters in this model, η, ζ and α_Z, and their dependences on mass (usually halo) and redshift. We take $\dot{M}_{\rm grav}$ from Dekel et al. (2009).

Our choices for these three baryon cycling parameters are guided by numerical simulations and observational results. We assume $\eta \propto M_{\rm halo}^{-2/3}$, as advocated by Behroozi, Wechsler & Conroy (2012) and, as we show in Fig. 1, results in a model stellar mass to halo mass ratio comparable to what is inferred from abundance matching. We take α_Z from a crude parametrization based on simulations of Davé, Oppenheimer & Finlator (2011)

$$(1-\alpha_Z)^{-1} = \mathrm{e}^{-Z} \left(\min(M_{\rm halo}/10^{12}\,\mathrm{M}_\odot, 1)\right)^{2/3}. \tag{13}$$

These analytic model choices approximately reproduce simulation results for key galaxy evolutionary properties such as the star formation history, metallicities and gas fractions.

For this work, a key issue is quenching, because as we will show, low-level star formation in massive galaxies *after* quenching is an important element of our model. We include a number of sources of preventive feedback in the model (ζ).

$$\zeta = \zeta_{\rm photo} \times \zeta_{\rm grav} \times \zeta_{\rm winds} \times \zeta_{\rm quench}, \tag{14}$$

where $\zeta_{\rm photo}$ represents heating of cold infalling gas by photoionizing radiation, and is principally important at low masses. Here, we use the parametrization advocated by Gnedin (2000) and Okamoto, Gao & Theuns (2008), such that $\zeta_{\rm photo} \propto [1 + 1/3(M/M_\gamma)^{-2}]^{-1.5}$ with M_γ given in Davé et al. (2012, fig. 1). $\zeta_{\rm grav}$ parametrizes the suppression of gas inflow owing to virial shocks, and is proportional to $(1+z)^{0.38} \times M_{\rm halo}^{-0.25}$ (Faucher-Giguère, Kereš & Ma 2011); while the simulations that determine this parametrization for $\zeta_{\rm grav}$ do not include metal line cooling, results with metal cooling from Davé et al. (2011) confirm this scaling. $\zeta_{\rm winds}$ represents the impact of energy input by winds, and scales as $\sim \mathrm{e}^{-\sqrt{M_{\rm halo}}}$ (Oppenheimer et al. 2010). Generally speaking, winds and photosuppression of infall do not impact the massive galaxies that concern us in this study.

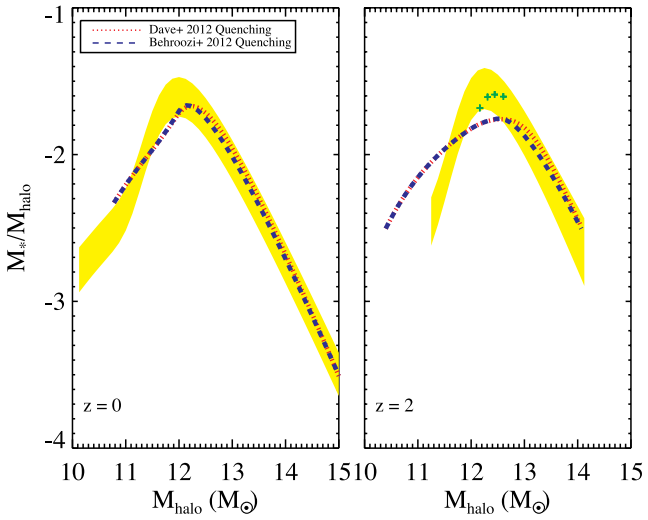

Figure 1. M_*–$M_{\rm halo}$ relation for model galaxies with the two quenching models employed in this work. The red and blue lines show the two different quenching models employed in this work, while the yellow band shows observational constraints presented by Behroozi, Wechsler & Conroy (2013) and Behroozi et al. (2012). The left-hand panel shows $z \sim 0$ galaxies, while the right shows galaxies at $z \sim 2$. The green crosses in the right panel show observational constraints by Wake et al. (2011). At low redshift, galaxies that form in our equilibrium model show excellent correspondence with observed galaxies. Beyond this, the different quenching models produce similar galaxies, owing to the fact that the bulk of stars are formed prior to quenching. At higher redshifts, the models may be discrepant from observations at low mass, though we note that observations of stellar mass functions at $z \sim 2$ are still relatively uncertain. In any case, the correspondence for massive galaxies (the galaxies that concern us in this work) is quite reasonable, even at high z.

$\zeta_{\rm quench}$ represents putative quenching mechanisms (e.g. feedback from an active galactic nucleus [AGN]) not encompassed in the other forms of feedback. For massive galaxy evolution, $\zeta_{\rm quench}$ tends to have the biggest impact on the SFH which can impact the exact form of the stellar IMF at $z \sim 0$ in our model. Here, we investigate our results in terms of two potential quenching models. For the first, we follow Davé et al. (2012), and model $\zeta_{\rm quench}$ with a similar functional form as $\zeta_{\rm photo}$, but with a characteristic mass of $M_{\rm q} = 10^{12.3}\,{\rm M}_\odot$. The second model appeals to recent work by Behroozi et al. (2012) which utilizes observational constraints on the stellar masses of galaxies to model the scaling between the cosmic star formation efficiency (cSFE)[5] and galaxy halo mass. Behroozi et al. (2012) find that the cSFE scales as $M_{\rm halo}^{-4/3}$. When parametrizing in terms of the stellar mass–halo mass relation, the threshold halo mass beyond which the cSFE becomes inefficient is $\sim M_{\rm halo} \gtrsim 10^{12}\,{\rm M}_\odot$. Because $\zeta_{\rm grav}$ dominates over $\zeta_{\rm photo}$ and $\zeta_{\rm winds}$ for massive galaxies, including a quenching term $\zeta_{\rm quench} \propto M_{\rm halo}^{-1.083}$ for halo masses $M_{\rm halo} > 10^{12}\,{\rm M}_\odot$ results in a cSFE in our models that scales with $M_{\rm halo}^{-4/3}$, per the constraints of Behroozi et al. (2012).

The galaxies that result from the two quenching models are reasonably similar. In Fig. 1, we plot the $z = 0$ stellar mass–halo mass relation for the galaxies in both quenching models. Owing to the fact that the bulk of the stellar mass is built up prior to quenching, the two models result in quite similar M_*–$M_{\rm halo}$ relations. As we will show, while the low-level star formation history at late times can affect the present-day stellar IMF in our model, for plausible choices of the SFH, the results are qualitatively similar.

This equilibrium model for the cosmological evolution of galaxies does not account for galaxy mergers. While merger-driven starbursts do little to contribute to the total stellar mass of a galaxy (e.g. Rodighiero et al. 2011), the added stellar content can affect the observed properties (e.g. the M/L ratio) if the merger is close to equal mass. Hence we explicitly include additional growth owing to galaxy mergers.

We estimate the galaxy–galaxy merger rate from the publicly available model developed in Hopkins et al. (2010). Briefly, we calculate halo mass functions and merger rates at a given redshift from the Millennium simulation (Fakhouri, Ma & Boylan-Kolchin 2010), and assign galaxies to these haloes following a standard halo occupation formalism (Conroy & Wechsler 2009). After correcting for the dynamical friction time-delay between halo–halo and galaxy–galaxy mergers (Boylan-Kolchin, Ma & Quataert 2008), we then have a galaxy merger rate as a function of galaxy mass and redshift. The mapping between galaxy mass and halo mass is dependent on knowing the galaxy mass function as a function of redshift. For this, we utilize observed galaxy mass functions. From $z = 0$–2, we utilize the mass functions from Arnouts et al. (2007) and Ilbert et al. (2010) as bracketing the range of observed mass functions. At $z > 2$ we utilize mass functions from Pérez-González et al. (2008) and Marchesini et al. (2009). The principle effect of including galaxy mergers is to add to the uncertainty present in trends as the uncertainty in high-z galaxy mass functions dominates the uncertainty in these models. This said, as we discuss later, the trends presented in this work are robust, and only the normalization tends to vary with different mass function choices. We have run versions of our model with each of the aforementioned mass functions, and discuss the range of uncertainty as we present our results.

The combination of simple but realistic star formation histories for individual galaxies from the equilibrium model plus the merger history derived from the Millennium simulation allows us to quickly and effectively model the evolution of the galaxy population. This in turn enables us to efficiently examine the impact of IMF variations parametrized by SFR and metallicity on galaxy properties.

3 RESULTS

3.1 Summary of cloud thermal state and scaling of IMF with galaxy physical properties

Because the methods described in Section 2.3 dictating the thermal state of the clouds are somewhat detailed, we find it useful to summarize the general trends in cloud temperatures with the intent of giving the reader an intuition for the different physical processes that determine the temperature in different regimes.

Without any sources of heating, the cloud temperatures would cool to the microwave background temperature. The dominant sources of heating are gas–dust coupling when the GMC is at high density ($n \gtrsim 10^4\,{\rm cm}^{-3}$), and cosmic ray heating at lower densities ($n \lesssim 10^2\,{\rm cm}^{-3}$).

At high densities, the energy exchange between gas and dust becomes extremely efficient. In heavily star-forming systems, the gas temperature is, to the first order, set by the dust temperature due to large fractions of dense gas (e.g. Juneau et al. 2009). While

[5] That is the galaxy SFR divided by the halo accretion rate. This is to be distinguished from either the mass of stars formed divided by the total mass in a molecular cloud [$M_*/(M_* + M_{\rm cloud})$], or the SFR/$M_{\rm H2}$ (i.e. an inverse time-scale), both of which are also commonly referred to as the star formation efficiency.

cosmic rays can play a significant role in high SFR galaxies (e.g. Papadopoulos 2010; Papadopoulos et al. 2011), in these models energy exchange with dust plays a comparable or greater role in setting the gas temperature (Narayanan et al. 2012a). Because the dust temperature rises with the SFR (e.g. Narayanan et al. 2010b), the gas temperature does as well.

In low SFR systems, the mean gas density is relatively low. Here, cosmic rays determine the gas temperature. For a galaxy forming stars at a rate similar to the Galaxy ($\sim$2 $M_\odot$ yr^{-1}), the resulting temperature is $\sim$10 K, comparable to observations of Galactic clouds (Blitz et al. 2007; Fukui & Kawamura 2010). At lower SFRs, the cloud temperature can drop below this value.

The cloud Jeans mass, which scales as $T^{3/2}/n^{1/2}$ therefore scales, on average, with the galaxy-wide SFR. Physically, this dependence arises from gas–dust coupling at high densities (combined with increasing dust temperatures with increasing SFRs), and the scaling of cosmic ray fluxes with SFRs at lower densities. Utilizing the information from the $\sim 10^3$ galaxy snapshot realizations modelled here (again, the entire parameter space surveyed is listed in table A1 of Narayanan et al. 2012a), we fit the relationship between the H_2 mass-weighted Jeans mass in our model galaxies and the galaxy SFR. The H_2 mass-weighted Jeans mass is calculated by weighting the Jeans mass of each cell by the H_2 mass present, and the Jeans mass is calculated utilizing the median gas density in the cell (i.e. the density above which half the mass resides). The median density is calculated assuming the gas has a lognormal density distribution function, with width given by equation (1). This results in a relation:

$$M_{\rm J} \sim {\rm SFR}^{0.3}\,{\rm M}_\odot \tag{15}$$

with a normalization set at a Galactic SFR of 2 $M_\odot$ yr^{-1}.

Under the Jeans conjecture, the scaling of the average Jeans mass of molecular clouds has implications for the stellar IMF. We assume the IMF has a similar basic shape in all galaxies, and takes the form of a Kroupa broken power law with a low-mass slope of 0.3, and high-mass slope of -1.3 [where the IMF slope specifies the slope of the $\log_{10}({\rm d}N/{\rm d}\log M)$–$\log_{10}({\rm M})$ relation]. For Milky Way conditions, the turnover mass, $M_{\rm c}$, is set to 0.5 $M_\odot$, and varies with the SFR for other galaxies. Thus, for IMF variations, we have

$$M_{\rm c} = 0.5 \times \left[\frac{\rm SFR}{\rm SFR_{MW}}\right]^{0.3}. \tag{16}$$

Under the Jeans conjecture, the IMF therefore varies with the conditions in the ISM. Physically, the IMF tends towards top-heavy in heavily star-forming galaxies due to efficient energy exchange between gas and dust in dense environments. Conversely, the IMF tends towards bottom-heavy in poorly star-forming galaxies owing to decreased cosmic ray fluxes. It is important to note that the *shape* of the IMF does not change in this model – only the turnover mass. To explicitly show this point, in Fig. 2, along with a standard Salpeter and Kroupa IMF, we show example IMFs for a low-SFR bottom-heavy system ($M_{\rm c} = 0.25\,{\rm M}_\odot$), and a high-SFR top-heavy system ($M_{\rm c} = 1\,{\rm M}_\odot$).

As we will see, equation (16) combined with the results from Section 2.4 prepare us to analyse the cosmic evolution of the IMF under the assumption of the Jeans conjecture. Finally, we note that formally, the rise in Jeans masses in high-SFR galaxies can be modulated in very low metallicity environments owing to a metallicity-dependent dust–gas energy exchange rate (Krumholz et al. 2011). Typically, heavily star-forming systems do not remain metal-poor in our model for very long, however, and any metallicity-dependence in equation (16) has minimal impact on the IMF in massive galaxies at $z \sim 0$ under the Jeans conjecture. Future work will discuss the star formation properties of low-metallicity, heavily star-forming systems at high redshift.

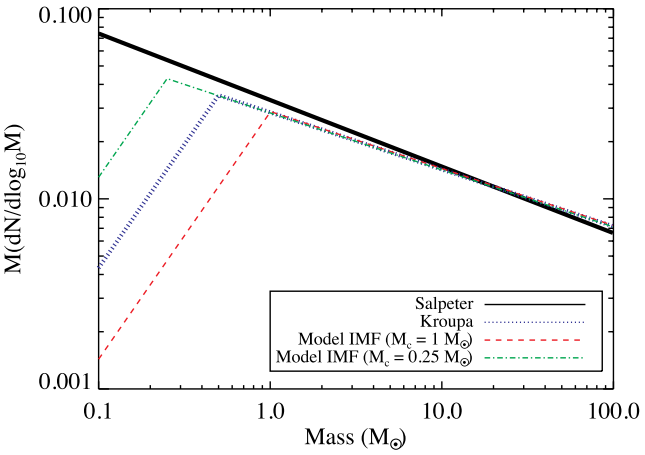

Figure 2. Example stellar IMFs. The black solid line denotes a standard Salpeter (1955) IMF, whereas the other three show Kroupa (2002) broken power-law forms. The blue dashed line is the typical Galactic Kroupa IMF with turnover mass $M_{\rm c} = 0.5\,{\rm M}_\odot$. The green dash–dotted line represents a bottom-heavy IMF (with $M_{\rm c} = 0.25\,{\rm M}_\odot$), while the red dashed line is a top-heavy IMF (with $M_{\rm c} = 1\,{\rm M}_\odot$). At solar metallicities, the bottom-heavy IMF may represent a galaxy forming stars at $\sim$0.2 $M_\odot$ yr^{-1}, while the top-heavy IMF is characteristic of a galaxy forming stars at $\sim$20–25 $M_\odot$ yr^{-1}. An important point is that the shape of the IMF does not change under the model assumption of the Jeans conjecture: only the turnover mass. The IMFs are normalized arbitrarily by the integral $\int M({\rm d}N/{\rm d}\log_{10}M)\,{\rm d}M$.

3.2 The meandering of the IMF over cosmic time

In Fig. 3, we plot the cosmic evolution of the halo mass, M_*, SFR, IMF characteristic mass (cf. Fig. 2), and K-band M/L ratio (normalized by what one would see for a standard Kroupa IMF) for three model galaxies for both quenching models. The model galaxies are chosen to have the same final stellar mass. We defer discussion of the M/L ratio evolution until Section 3.3.

The characteristic star formation history of galaxies is, to the first order, determined by the gas accretion rate from the IGM which is dictated by gravity. Fits to models from various groups all find accretion rates dependent on both the halo mass and redshift via $\dot{M}_{\rm grav} \propto M_{\rm halo}^{0.05-0.15} \times z^{2-2.5}$ (e.g. Dekel et al. 2009; Fakhouri et al. 2010; Faucher-Giguère et al. 2011).

In this picture, more massive galaxies on average have higher peak SFRs, and peak at earlier times (e.g. Noeske et al. 2007a,b). As an example, while a ($z = 0$) Milky-Way-sized halo peaks in SFR between $z = 0$ and 1, and has a peak SFR of $\sim$10–20 $M_\odot$ yr^{-1}, a galaxy in a ($z = 0$) $\sim 10^{14}$ $M_\odot$ halo peaks at $\sim$200–300 $M_\odot$ yr^{-1} at $z \sim$ 2–3. Neglecting metallicity effects (which only play an important role for the most part at redshifts $z \gtrsim 4$), the evolution in the turnover mass in the IMF broadly follows the star formation history. Turning to the third panel in Fig. 3, we now highlight the grey horizontal line which denotes the typical Kroupa turnover mass of $M_{\rm c} = 0.5\,{\rm M}_\odot$ in the Milky Way.

Massive galaxies that undergo heavy SFR periods at early times see an increase in their average cloud temperatures,[6] and hence an increase in the characteristic turnover mass in their stellar IMFs

[6] The cloud densities of course increase as well, but the Jeans mass goes as $M_{\rm J} \sim T^{3/2}/n^{1/2}$.

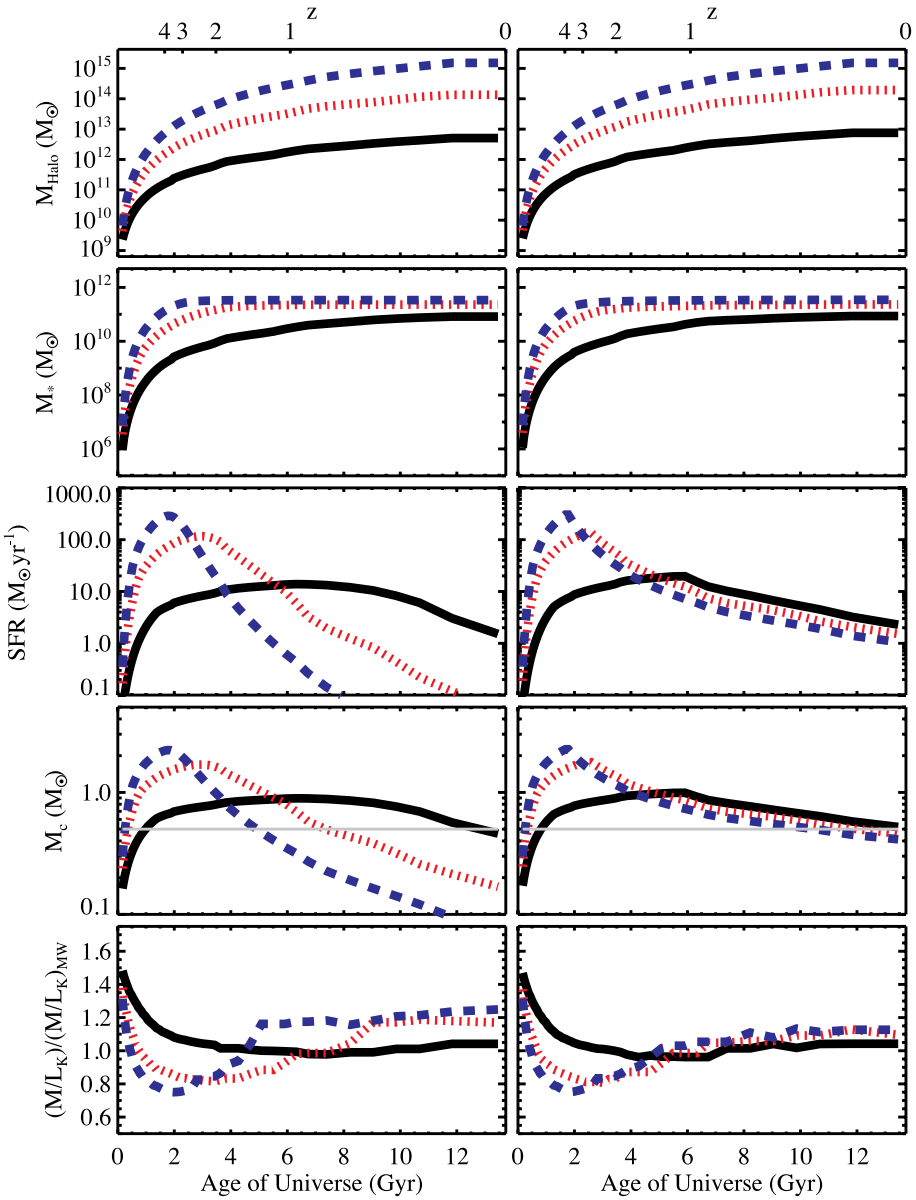

Figure 3. Cosmic evolution of model galaxy halo masses, M_*, SFRs, IMF turnover masses, and K-band M/L ratios for three galaxy masses. The left column shows the quenching model from Davé et al. (2012), while the right column shows the quenching model designed to match the constraints of Behroozi et al. (2012). The galaxies are picked to have the same final stellar mass for each quenching model. The thin grey line in the fourth panel denotes $M_c = 0.5\,M_\odot$, the turnover mass for a Galactic Kroupa IMF. The M/L ratios are normalized by the expected values for a Kroupa IMF to assist in comparing with observations (Conroy & van Dokkum 2012b). The small features in the M/L ratio owe to the discretization of the SFH into individual bursts, as well as galaxy mergers (see text for details). The IMF for a massive galaxy may vary over cosmic time from top-heavy to bottom-heavy as follows. During epochs of heavy star formation, the Jeans masses of clouds increase owing to gas in clouds heated by warm dust in dense environments. These galaxies may exhibit top-heavy IMFs under the Jeans conjecture. Galaxies of increasing mass peak in their cosmic star formation history at earlier times, and undergo long periods of star formation at rates below the Milky Way's. Decreased cosmic ray fluxes during low SFR periods result in cloud Jeans masses lower than typical Galactic values, and hence an excess of low-mass stars in their IMFs at late times.

at early times (e.g. top-heavy/bottom-light IMFs). In Narayanan & Davé (2012), we showed that the top-heavy IMF in high-z star-forming galaxies that results from a Jeans model can alleviate tensions associated with inferred SFRs from high-z galaxies.

As the SFRs of massive galaxies decline due to a combination of gas exhaustion and cosmic expansion of the Universe, so do their cosmic ray fluxes. Below $z \sim 2$, when the cosmic microwave background (CMB) temperature decreases below $T_{CMB} \lesssim 10$ K, the temperatures of the GMCs may decrease below the typical $\sim$10 K value seen in Milky Way clouds. Consequently, the cloud Jeans masses drop and the IMF becomes bottom-heavy. For the most massive galaxies we consider, the transition between top-heavy and bottom-heavy (defined as when the turnover mass in the IMF transitions from above $0.5\,M_\odot$ to below) happens at $z \sim 1$–2.

Under the Jeans conjecture, then, the IMF meanders over cosmic time, generally guided by the galaxy-wide SFR. The exact form of the meandering is galaxy mass-dependent. For example, the most massive galaxies ($M_{halo} \sim 10^{14}\,M_\odot$ at $z \sim 0$) peak in their SFR, and hence their IMF characteristic mass, at $z \sim 2$–4. They then go through a bottom-heavy phase for roughly half a Hubble time. It

is important to note, though, that the bulk of the stars that form during the galaxy's lifetime do so during the top-heavy phase. It is only *newly* formed stellar clusters that will exhibit a bottom-heavy IMF in massive galaxies at $z \sim 0$ under the assumption of the Jeans conjecture.

Galaxies that reside in Milky Way-sized haloes at $z \sim 0$ peak in their SFRs so late that they never undergo a bottom-heavy phase, and are only weakly top-heavy at late times ($z \lesssim 1$). Interestingly, galaxies that are much less massive than the Milky Way never have large ($\gtrsim$2 $M_\odot$ yr^{-1}) SFRs, and thus have bottom-heavy IMFs for the bulk of their lives in this model.

It is important to note short-term fluctuations in the cosmic evolution of the star formation history from a given galaxy can cause deviations in the IMF from the trends presented in Fig. 3 and discussed in this section. For example, a gas-rich major merger that drives an intense burst of star formation can temporarily drive up gas temperatures, and hence the cloud Jeans masses. This said, under the Jeans conjecture, on average the IMF trends will follow those shown in Fig. 3. We now expand upon the trends discussed here and compare more specifically to inferred measurements of the IMF from observations.

3.3 The mass-to-light ratio in $z = 0$ massive ellipticals

As discussed in the Introduction, various circumstantial arguments favour a bottom-light IMF in rapidly star-forming galaxies at high redshifts. Such arguments are detailed more thoroughly in Narayanan & Davé (2012), where we consider the implications of the Jeans mass conjecture on high-z galaxies. In Section 4.2 we discuss arguments for and against the interpretation of a bottom-light (or top-heavy) IMF in massive high-z galaxies. Here, we consider the implications of our varying IMF for the descendents of massive high-z galaxies, which today are expected to be early-type 'red and dead' ellipticals.

Observationally, a number of works have found that the K-band mass-to-light ratio (M/L_K) increases with stellar mass more quickly than expected for a standard Kroupa or Chabrier IMF (e.g. Treu et al. 2010; Cappellari et al. 2012a; Conroy & van Dokkum 2012a,b). Observationally, this is parametrized as an increase in M/L_K with galaxy velocity dispersion, σ.

What happens in our Jeans conjecture model? Referring again to Fig. 3, a trend in the characteristic IMF mass at $z \sim 0$ is apparent with increasing galaxy mass. While a Milky Way mass galaxy peaks in its SFR around $z \sim$ 1–2, and only settles to an IMF with $M_c \approx 0.5\,M_\odot$ around $z \sim 0$, more massive galaxies peak in their SFR at earlier times. These galaxies exhaust their fuel rapidly, are unable to replenish their gas owing to strong preventive feedback, and settle into a low SFR mode (perhaps in an episodic fashion) for up to $\sim$ half a Hubble time. By present epoch, the only signature of the massive stars that formed during the peak star formation event are their stellar remnants.

We employ stellar population synthesis models to derive the stellar mass-to-light ratio from our model galaxies. We utilize FSPS, a flexible, publicly available stellar population synthesis code described in Conroy et al. (2009, 2010) and Conroy & Gunn (2010). For a given galaxy, we utilize the star formation history and cosmic evolution of the IMF to evaluate the properties of the $z = 0$ stellar populations. We model a given galaxy by discretizing the star formation history into a series of bursts. We run FSPS assuming the star formation history is a single burst at each redshift, with the corresponding M_c derived from our Jeans model. We then sum the

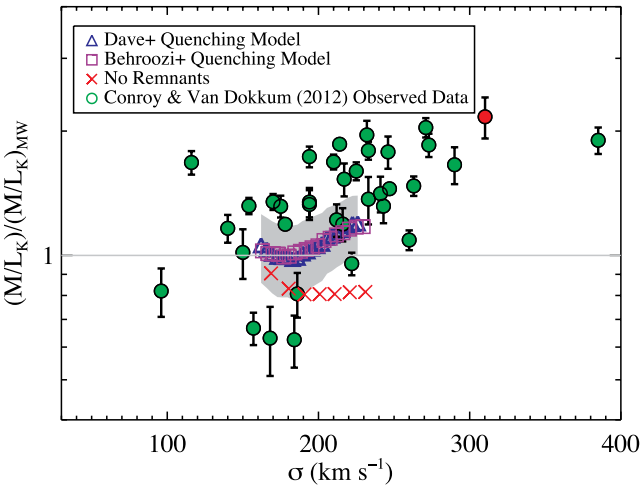

Figure 4. Stellar mass to (K-band) light ratios as a function of galaxy stellar velocity dispersion for simulated galaxies (blue triangles and purple squares), and observed galaxies (green and red circles with error bars; Conroy & van Dokkum 2012b). The blue triangles have SFHs with the Davé et al. (2012) quenching model imposed, while the purple squares have a quenching model designed to match constraints on the cSFE–M_{halo} relation from Behroozi et al. (2012). The M/L_K ratios are normalized by what is expected from a Kroupa IMF. The grey shaded region denotes a 0.2 dex uncertainty in the normalization of the models (see text for details). Galaxies of increasing mass have larger SFRs at earlier epochs. Due to stellar remnants that remain from massive stellar evolution, the observed M/L ratios are higher at present epoch. See text for details.

M/L ratios, weighting by the stellar masses, of the galaxy over its cosmic history to determine the M/L ratio at a given redshift.

We now refer to the bottom panel of Fig. 3. Here, we show M/L_K normalized by what is expected from a standard Kroupa IMF. The masses include the contribution from stellar remnants (e.g. white dwarfs and neutron stars). As is evident, a galaxy residing in a Milky Way sized halo at $z \sim 0$ has a M/L_K ratio comparable to what is expected from a standard Kroupa IMF. Galaxies of increasing mass have increasingly large M/L_K ratios.

This trend is more clearly seen in Fig. 4, where we examine the \$z\$ = 0 M/L ratios in our model galaxies against stellar velocity dispersion (serving as a proxy for galaxy mass). To remain consistent with the way observations are presented, we normalize M/L_K by a Milky Way ratio (here, a Kroupa IMF with $M_c = 0.5\,M_\odot$; C. Conroy, private communication). The velocity dispersion is calculated utilizing fits to the dynamical mass versus velocity dispersion from Sloan Digitized Sky Survey (SDSS) galaxies presented in van de Sande et al. (2011).

The blue triangles and purple squares in Fig. 4 denote the individual galaxy realizations from the cosmological simulations. The overall normalization of the simulated points is not very robust against our model assumptions. Variables such as the assumed Galactic SFR (which dictates when decreased cosmic ray fluxes will allow cloud temperatures to drop below $\sim$10 K) and the assumed stellar mass function at high-redshift (which can affect the galaxy merger rate; cf. Section 2.4) can slightly change the normalization of the M/L_K ratio as a function of mass. Varying these parameters within reasonable bounds changes the M/L_K ratios is $\sim$0.2 dex and this region of uncertainty is highlighted by the grey shaded region (only noted for the Davé quenching model). The magnitude of the trend in M/L_K with σ depends on the exact form the SFH (and

hence the quenching model). This said, for plausible star formation histories, a general trend of increasing M/L_K ratio with σ is evident.

The points with error bars show data from the observational work of Conroy & van Dokkum (2012b). The green points are a sample of nearby early-type galaxies (including the bulge of M31), and the red point is stacked data from four galaxies in the Virgo cluster. The data show increasing M/L ratios with increasing stellar velocity dispersion. Similar trends have been noted by Treu et al. (2010); Smith et al. (2012) and Cappellari et al. (2012a) as well. The model results are qualitatively in agreement with observational data. They indicate that galaxies with σ typical of the Milky Way represent a minimum in the M/L ratio in our Jeans conjecture IMF relative to a Kroupa IMF. Galaxies of increasing mass (or velocity dispersion) show increasing M/L ratios.

The M/L_K ratio increases with galaxy velocity dispersion due to the increased contribution from stellar remnants in our models. Galaxies of increasing mass have undergone increasingly bottom-light phases at earlier times, and thus have larger contributions to their stellar masses at present epoch by stellar remnants.

Galaxies at lower velocity dispersions, in this model, also tend to have increased M/L ratios. In these galaxies, the stellar population is actually bottom-heavy. This result comes from the protracted epoch of low star formation associated with massive galaxies that populate the low-mass end of the IMF at late times, while in low-mass galaxies (which are typically still star-forming today) the low SFRs and metallicities result in a bottom-heavy IMF at all times.

When comparing to observations, two salient points arise. First, while the M/L ratio increases with increasing galaxy mass in our model, this is due to stellar remnants from the top-heavy phase, not an increasingly bottom-heavy IMF. This is seen more explicitly via the red crosses in Fig. 4, where we plot the M/L ratio of our models with the effects of stellar remnants turned off in the SPS calculations. The shape of M/L with σ for the case of no remnants owes to a competition between lack of stellar remnants in high-mass galaxies with increasingly bottom-heavy IMF's at late times.

Still, the correspondence of our fiducial model with observations is reasonable. Many of the observational studies aimed at understanding the IMF in galaxies infer the IMF indirectly by constraining the M/L ratio. If the Jeans hypothesis is correct, then the observed increase in M/L_K ratio with galaxy mass owes to a prior top-heavy phase, rather than bottom-heavy phase. The two scenarios are degenerate in terms of observed M/L ratios. This said, measurements of gravity-sensitive stellar absorption features by groups such as Conroy & van Dokkum (2012b) and others directly probe the stellar IMF within the central regions of galaxies. If indeed the IMF is bottom-heavy as these studies imply, this may provide difficulty for the Jeans model.

Secondly, in detail, this model cannot attain the approximately two times increase in M/L_K relative to Kroupa as seen in some galaxies, including the stack of Virgo ellipticals (red point). It may be possible to tweak model parameters to achieve this. For instance, we have assumed that the IMF form is always Kroupa-like; if instead the IMF also had a shift to a shallower slope, this would result in more massive stars that would disappear by today, and would increase the relative contribution of the low-mass stars created during the low-SFR phases of evolution, when the IMF was more bottom-heavy.

Galaxy mergers moderately enhance the M/L ratio in massive galaxies. This is because in our model, low-mass galaxies have a bona fide (slightly) bottom-heavy IMF as they never achieve significant periods of star formation above $\mathrm{SFR_{MW}}$. The massive galaxies of course have a large M/L due to the presence of remnants. As a result, mergers with low-mass galaxies can add more low-mass stars and slightly increase the observed M/L_K ratio. This said, we do not account for the increased SFR driven by galaxy mergers. Qualitatively, one would expect to observe a top-heavy IMF in an ongoing merger due to increased SFRs and hence Jeans masses (via increased gas temperatures). A complete accounting of all these effects would require implementing a full evolutionary IMF model within a cosmologically based galaxy formation model that includes the effects of mergers self-consistently; we leave this for future work.

4 DISCUSSION

In Narayanan & Davé (2012) we discussed the implications of an IMF following the Jeans conjecture on the properties of high-redshift star-forming galaxies. We showed that this IMF goes significantly towards alleviating a number of difficulties in understanding the evolution of the SFR–M_* relation and sub-millimetre galaxies, and has interesting implications for the star formation law.

In this paper we consider the implications of the Jeans conjecture on the evolution of passive, massive galaxies. While our main focus is their M/L ratios, there are a number of other implications for massive galaxies that we now briefly consider.

4.1 Galaxy star formation and chemical enrichment history

For a typical massive galaxy in this model, the star formation history peaks at high-redshift, and once the halo mass exceeds the quenching mass M_{quench} its star formation begins to become strongly suppressed (see fig. 1 of Davé et al. 2012). The physical mechanism for this is purported to be AGN feedback (e.g. Croton et al. 2006), although our model is purely parameteric. The resulting star formation histories for different quenching models are shown in Fig. 3: more massive galaxies have earlier and higher peaks of star formation, consistent with stellar population data for early-type galaxies (Thomas et al. 2005), and reminiscent of the observationally derived 'staged' galaxy formation model (Noeske et al. 2007a,b). Importantly, the SFR remains finite, albeit small, even after quenching has kicked in. This SFH integral is important for driving top-heavy IMFs in galaxies during high SFR epochs, and the observed M/L ratio in present-epoch galaxies.

The star formation histories presented here are broadly consistent with observations. Recent studies find that low levels of star formation and dense molecular gas are widespread among $z \sim 0$ early-type galaxies (Xu, Narayanan & Walker 2010; Crocker et al. 2011; Young et al. 2011; Davis et al. 2011; Crocker et al. 2012), Additionally, observations by the ATLAS^{3D} collaboration appear to tentatively suggest that ellipticals have star formation histories consistent with those presented here, with more massive galaxies typically having older stellar populations (McDermid et al. 2012). In this sense, that our model suggests that more massive galaxies peak in their SFH at increasingly early times, followed by low-level residual star formation may be reasonable.

While early-type galaxies clearly undergo some small levels of star formation, there is significant variance in the amount of star formation among galaxies, suggesting a duty cycle for this 'frosting' of star formation. In our simple model, this would result in a less bottom-heavy M/L_K, because the actual SFRs would be higher (albeit over shorter periods of time). However, this would not result in a change in the *trend* of M/L_K unless there was a systematic variation in the duty cycle with σ.

Another issue relates to the chemical enrichment history of ellipticals, which can be significantly impacted by changes in the

IMF. Galaxies with short star formation time-scales are expected to have enhanced [α/Fe] ratios. This is because when star formation is burst-like, the enrichment is dominated by Type II supernovae, thus the stars will be enhanced in elements that are products of the α process in stellar evolution. On the other hand, when star formation occurs over an extended period, there is time for Type Ia supernovae to contribute Fe to the chemical makeup of the galaxy. Observationally, more massive galaxies appear to be more α-enhanced (Trager et al. 2000). Arrigoni et al. (2010) showed that more top-heavy mass functions will increase the [α]/Fe ratios in galaxies, and that top-heavy models may be needed to match the observed enrichment trends. Without introducing a full chemical evolution model (and its associated uncertainties) to these simulations, however, being more quantitative is currently infeasible.

In summary, observations show both evidence for ongoing star formation in early-type galaxies (Crocker et al. 2011), older stellar populations on average for more massive galaxies (Thomas et al. 2005; McDermid et al. 2012; Pacifici et al. 2012) and increasing [α/Fe] ratios in early types (Trager et al. 2000), suggesting that the typical star formation histories calculated by our cosmological galaxy evolution model may not be unreasonable. However, current uncertainties in the detailed SFH and chemical enrichment histories of early-type galaxies are such that these issues cannot definitely confirm or rule out a Jeans conjecture origin for the bottom-heavy IMF in ellipticals.

4.2 Is the IMF in rapidly star-forming galaxies top-heavy?

The Jeans conjecture IMF model predicts that ellipticals undergo an early bottom-light/top-heavy phase during its peak SFR epoch. Narayanan & Davé (2012) have suggested that this may go some distance towards alleviating a number of difficulties in understanding the evolution of high-z galaxies. In the Jeans model, newly formed clusters in a present epoch massive galaxy will form in a bottom-heavy fashion, though the bulk of the stars formed over cosmic time will have done so in a bottom-light fashion.

Other works have investigated the potential for a top-heavy IMF in massive starbursts. For example, Weidner, Kroupa & Pflamm-Altenburg (2011) have investigated the effects of crowding of cloud cores in GMCs, and found that the integrated galactic IMF may become top-heavy when the galaxy SFR is $>10\,\mathrm{M}_\odot\ \mathrm{yr}^{-1}$ (see also Kroupa et al. 2013).

There is, alternatively, a general class of models that aims to understand the origin of the bottom-heavy IMF in ellipticals by making the IMF more bottom-heavy during phases of heavy starbursts. Bate (2009) and Krumholz (2011) examined the role of radiative pressure in setting the characteristic mass of the IMF. Krumholz showed that if the characteristic mass is set by radiative feedback from young protostars, then the IMF will scale very weakly with pressure such that in high-pressure systems (i.e. the heavily star-forming galaxies that serve as the progenitors for local early-types) a bottom-heavy IMF results. Similarly, Hopkins (2012) showed that if the IMF is set by the sonic mass in gas, rather than the Jeans mass, then starbursts will show an excess of low-mass stars. While neither model directly examines the observable properties of a $z \sim 0$ early-type galaxy population, it is likely that they too would show an excess of low-mass stars in accordance with observations. In this sense, whether the IMF is top-heavy or bottom-heavy in starburst systems may be a discriminant in general classes of IMF models. It is therefore worth examining claims of top-heavy IMFs in high SFR systems critically.

A number of studies have noted a mismatch between the observed cosmic evolution of stellar mass density and cosmic SFR density such that the inferred SFR density produces a factor of $\sim$2 more stars at $z \sim 0$ than are measured (Hopkins & Beacom 2006; Wilkins, Trentham & Hopkins 2008). While Narayanan & Davé (2012) showed that an IMF that varies with the Jeans masses in galaxies could go some distance towards reconciling these differences (producing only a mismatch in the stellar masses at $z \sim 0$ of a factor of 1.3 instead of 2), some observational studies either fail to find such a mismatch (e.g. Sobral et al. 2012), or propose non-IMF based solutions to the apparent discrepancy (Reddy & Steidel 2009; Stark et al. 2012).

Another commonly invoked candidate for a top-heavy IMF in starburst galaxies is the most heavily star-forming galaxy population in the Universe, the $z \sim 2$ submillimetre-selected population. The arguments are primarily theoretical. Simply, most standard galaxy formation models have been unable to account for the full observed distribution of SMGs without resorting to a top-heavy IMF. The most extreme example was reported by Baugh et al. (2005) who suggested a flat IMF may be necessary to reconcile the observed SMG number counts, Lyman-break galaxy population and present-day stellar mass function. However, recent numerical simulations by Hayward et al. (2010) and Hayward et al. (2012b) show that if one accounts for a combination of effects, including small-scale dust obscuration in highly resolved simulations, the contribution of isolated galaxies and the contribution of galaxy pairs, the observed SMG number counts may be accounted for even under the assumption of a standard Kroupa IMF.

van Dokkum (2008) utilized the fact that the luminosity and colours of a galaxy may evolve differently, depending on the IMF, and found that a bottom-light/top-heavy IMF best fit the evolution of the M/L_B and $U-V$ colours for $0 < z < 1$ early-type galaxies in clusters. However, when accounting for potential variations in population synthesis models, frosting of young stellar populations in the galaxies (Trager, Faber & Dressler 2008), and the structural evolution of galaxies (Holden et al. 2010), van Dokkum & Conroy (2012) found that the same observations could be consistent with a Salpeter IMF.

Other evidence for bottom-light IMFs in heavily star-forming galaxies come based on an analysis of Hα equivalent widths and optical colours of $\sim$33 000 galaxies in the Galaxy and Mass Assembly (GAMA) survey (Gunawardhana et al. 2011). Similarly, comparisons of Hα to UV luminosity ratios have suggested more top-heavy IMFs in more heavily star-forming galaxies (Lee et al. 2009; Meurer et al. 2009), though at least some of these results may be explained via stochasticity in the formation of massive stars (Fumagalli, da Silva & Krumholz 2011) or variable star formation histories (Weisz et al. 2012).

In general, the purported IMF variations towards top-heavy are all fairly mild, and while it is tempting to solve a number of apparent problems at high-z with a mild shift in the IMF towards bottom-light/top-heavy, there could be other explanations for each of these observations. This said, it is interesting that all inferred IMF variations in heavily star-forming systems go in the direction of being more top-heavy/bottom-light. Whether heavily star-forming galaxies have a top-heavy or bottom-heavy IMF should be a direct discriminant between general classes of IMF theory.

In principle, one could use remnants to potentially distinguish whether the IMF for massive galaxies has gone through a top-heavy phase at early times. If galaxies undergo a top-heavy phase, then their dynamical masses will have a larger contribution from stellar remnants. This may be consistent with observed fractions of

low-mass X-ray binaries in ellipticals (e.g. Kim et al. 2009). On the other hand, if the bulk of the stellar mass is built up in a bottom-heavy phase, then the contribution from remnants to the dynamical mass will be minimal. Offsets between direct M/L measurements from stellar spectral features (which measure the masses of living stars) and dynamical modelling that includes the effect of remnants may potentially provide a constraint on this model.

The main idea of this paper is that the M/L ratios in today's ellipticals is consistent with a top-heavy IMF at earlier times in heavily star-forming systems under a Jeans model for the IMF. This is due to increased stellar remnants. Newly formed clusters in fact form in a bottom-heavy fashion in this model, though do not comprise the majority of the stellar mass. If the IMF is truly bottom-heavy in massive galaxies (as recent results from stellar absorption line spectra suggest), then this poses a challenge for the Jeans conjecture, and a bottom-heavy IMF at all epochs would more straightforwardly solve the problem (of course, at the cost of potentially exacerbating possible issues with high-redshift galaxies). Observations that distinguish whether the IMF varies in heavily star-forming systems, or as a function of formation age (e.g. Zaritsky et al. 2013), may prove to be a valuable model discriminant.

Weidner et al. (2013) present a toy model in which they allow the IMF switch from bottom-light to bottom-heavy early during the SFH of a representative galaxy. This sort of model is able to both reproduce the observed chemical enrichment of massive galaxies, as well as the potential bottom-heavy nature of their IMF. While this model does not self-consistently explain *why* the IMF should switch rapidly from bottom-light to bottom-heavy, it does give some insight as to what the timing for IMF changes should look like during a galaxy's SFH. If the IMF of heavily star-forming galaxies is truly bottom-light, and of their remnants, bottom-heavy, then the Weidner et al. (2013) toy model serves as a guide for constraining when and how rapidly the IMF needs to change to match observed constraints.

4.3 The validity of the Jeans conjecture

The most basic arguments surrounding the Jeans conjecture is that it is not entirely clear what scale one should average over in order to derive the physical conditions in the cloud. In this work, we assume that the IMF scales with global cloud properties, on scales of $\sim$70 pc. If one were to choose significantly smaller scales, as an example, it is possible that the temperature and density would not vary in a manner that kept the Jeans mass constant. A number of works have posited that a reasonable choice for scale may be one where the isothermality of the cloud is broken. Larson (2005) suggested that this is when the gas becomes energetically coupled to the dust, though other works have argued that the isothermality may be broken due to radiative feedback (Bate 2009; Krumholz 2011).

While we cannot resolve these scales, what likely matters most is not the physical conditions in GMCs as a whole, but rather the clumps that form stellar clusters. Our model follows the typical enhancements and decrements of the Jeans mass on cloud-wide scales given the physical conditions in a galaxy. So long as the physical conditions in star-forming clumps within a GMC scale in a self-similar manner with the global physical properties of the molecular cloud, then the galactic environment may indeed play a role in setting the fragmentation scale that impacts the distribution of core masses.

From a simulation standpoint, some tentative evidence exists that suggests a close connection between the cloud Jeans masses and IMF. Work by Bate & Bonnell (2005) and Klessen et al. (2007) showed that the mass spectrum of collapsed objects varies with the Jeans properties of the simulated cloud, and that conditions comparable to starbursts may have turnover masses as large as $\hat{M}_{\rm c} \approx 15\,{\rm M}_{\odot}$. This said, the degree of fragmentation is dependent on the exact form of the equation of state, and the scaling of the turnover mass may depend on the numerical resolution for isothermal simulations.

Perhaps the most convincing observational evidence for the Jeans conjecture is that it is reasonably well-established that the stellar IMF corresponds well with the cloud core mass function in some GMCs (André, Ward-Thompson & Motte 1996; Johnstone et al. 2001; Motte et al. 2001; Nutter & Ward-Thompson 2007; André et al. 2011). If these cores are the result of clump fragmentation that lead to star formation (Evans 1999; Lada & Lada 2003; Kennicutt & Evans 2012), then a relationship between the characteristic fragmentation scale and the IMF is natural. There is additionally some evidence from the Taurus star-forming region and Orion nebula Cluster that suggest variations in the IMF with cloud density in a manner that is consistent with a Jeans scaling (Briceño et al. 2002; Luhman et al. 2003; Luhman 2004; Da Rio et al. 2012), though the dynamic range of physical conditions on global cloud scales in the Galaxy is limited enough that unambiguous evidence for an IMF that varies with cloud Jeans masses is not yet present. ALMA observations will allow for better measurements of the relationship between GMC properties and core mass functions over a range of physical conditions which may shed light on the potential relationship between the stellar IMF and cloud Jeans mass.

Whether the IMF varies with the Jeans properties of clouds, or at all with gas physical conditions, remains an open question. While some observations show mild variations, unambiguous evidence for systematic variations are lacking (Bastian et al. 2010). The Jeans conjecture equally enjoys its share of tentative observational evidence, as well as contends against cogent theoretical arguments. In this work, we remain agnostic as to the validity of the Jeans conjecture, but rather simply aim to understand the potential consequences of an IMF that scales with global cloud properties.

5 SUMMARY

Utilizing a combination of hydrodynamic galaxy evolution simulations, a radiative model for the ISM and cosmological models for the star formation histories of galaxies, we investigate the cosmic evolution of the stellar IMF under the assumption that the IMF varies with the Jeans masses of molecular clouds in galaxies.

The IMF can be both top heavy and bottom heavy (at different times) for massive galaxies. At early times, the ISM is warm owing to the heating of dust by stars, and energy exchange between gas and dust. This drives Jeans masses in molecular clouds up, and, under the Jeans conjecture, results in a top-heavy IMF.

As galaxies evolve towards present epoch, their SFRs drop below Milky Way values, and a lack of cosmic rays allows the temperature of the ISM to cool below the $\sim$10 K characteristic of Galactic clouds. At these late times, the typical Jeans masses of clouds decrease, and the IMF tends towards an excess of low-mass stars (bottom-heavy). Newly formed stellar clusters in present-epoch massive galaxies will form with a bottom-heavy IMF under the Jeans conjecture. This said, the majority of stars formed will have done so in a top-heavy phase, and are thus challenged by stellar absorption-line measurements that suggest that massive galaxies at $z \sim 0$ have IMFs that are increasingly bottom-heavy with σ.

More massive galaxies form a larger number of stellar remnants during their top-heavy phases, and thus have increased M/L ratios. After convolving our models with stellar population synthesis

calculations, we find that the resultant M/L ratio for massive ellipticals increases with increasing galaxy mass. Given plausible galaxy star formation histories, a Jeans model for IMF variations provides a reasonable match to observed M/L–σ relations for observed elliptical galaxies at $z \sim 0$.

In short, by exploring the ansatz that the stellar IMF varies with the Jeans properties of clouds galaxies, we conclude that a Jeans model for IMF variations in galaxies is able to simultaneously reproduce the observed M/L ratios of present epoch massive galaxies, while motivating top-heavy IMFs at early times that may help alleviate some tensions in high-z galaxy evolution. The Jeans model suggests that increased M/L ratios in present-epoch massive galaxies owe to stellar remnants. If the IMF in massive galaxies is truly bottom-heavy, as gravity-sensitive spectral absorption features may indicate, then the Jeans conjecture may not be valid.

We remain agnostic as to the underlying Jeans assumption, as well as regarding inferred IMF variations at both low and high z. Improving constraints on the IMF in starbursting systems and confirming preliminary trends of varying IMF with star cluster age would seem to provide viable paths towards discriminating the Jeans conjecture model versus models that invoke bottom-heavy IMFs throughout the lifetime of today's massive galaxies.

ACKNOWLEDGEMENTS

DN thanks Peter Behroozi, Charlie Conroy, Phil Hopkins, Mark Krumholz, Richard McDermid, Daniel Stark, Rachel Somerville, Jesse van de Sande and Pieter van Dokkum for interesting and helpful conversations. We additionally thank Peter Behroozi, Charlie Conroy and David Wake for providing the data from their papers in digital format. We thank the referee for numerous suggestions that improved this work. This work benefited from work done and conversations had at the Aspen Center for Physics. DN acknowledges support from the NSF via grant AST-1009452. RD is supported by the National Science Foundation under grant numbers AST-0847667 and AST-0907998, and by NASA under grant number NNX12AH86G. Computing resources were obtained through grant number DMS-0619881 from the National Science Foundation.

REFERENCES

Abdo A. A. et al., 2010, ApJ, 709, L152
Acciari V. A. et al., 2009, Nat, 462, 770
Adams F. C., Fatuzzo M., 1996, ApJ, 464, 256
André P., Ward-Thompson D., Motte F., 1996, A&A, 314, 625
André P., Men'shchikov A., Könyves V., Arzoumanian D., 2011, in Röllig M., Simon R., Ossenkopf V., Stutzki J., eds, EAS Publications Series. Vol. 52, p. 167
Arnouts S. et al., 2007, A&A, 476, 137
Arrigoni M., Trager S. C., Somerville R. S., Gibson B. K., 2010, MNRAS, 402, 173
Auger M. W., Treu T., Gavazzi R., Bolton A. S., Koopmans L. V. E., Marshall P. J., 2010, ApJ, 721, L163
Bastian N., Covey K. R., Meyer M. R., 2010, ARA&A, 48, 339
Bate M. R., 2009, MNRAS, 392, 1363
Bate M. R., Bonnell I. A., 2005, MNRAS, 356, 1201
Baugh C. M., Lacey C. G., Frenk C. S., Granato G. L., Silva L., Bressan A., Benson A. J., Cole S., 2005, MNRAS, 356, 1191
Behroozi P. S., Wechsler R. H., Conroy C., 2012, ApJ, 762, L31
Behroozi P. S., Wechsler R. H., Conroy C., 2013, ApJ, 770, 57
Bigiel F., Leroy A., Walter F., Brinks E., de Blok W. J. G., Madore B., Thornley M. D., 2008, AJ, 136, 2846
Blitz L., Fukui Y., Kawamura A., Leroy A., Mizuno N., Rosolowsky E., 2007, in Reipurth B., Jewitt D., Keil K., eds, Protostars and Planets V. University of Arizona Press, Tucson, p. 81
Bolatto A. D., Leroy A. K., Rosolowsky E., Walter F., Blitz L., 2008, ApJ, 686, 948
Bondi H., Hoyle F., 1944, MNRAS, 104, 273
Boylan-Kolchin M., Ma C.-P., Quataert E., 2008, MNRAS, 383, 93
Brewer B. J. et al., 2012, MNRAS, 422, 3574
Briceño C., Luhman K. L., Hartmann L., Stauffer J. R., Kirkpatrick J. D., 2002, ApJ, 580, 317
Bullock J. S., Kolatt T. S., Sigad Y., Somerville R. S., Kravtsov A. V., Klypin A. A., Primack J. R., Dekel A., 2001, MNRAS, 321, 559
Calura F., Pipino A., Matteucci F., 2008, A&A, 479, 669
Cappellari M. et al., 2012a, MNRAS, 432, 1862
Cappellari M. et al., 2012b, Nat, 484, 485
Chabrier G., 2003, PASP, 115, 763
Chomiuk L., Povich M. S., 2011, AJ, 142, 197
Christensen C., Quinn T., Governato F., Stilp A., Shen S., Wadsley J., 2012, MNRAS, 425, 3058
Conroy C., Gunn J. E., 2010, ApJ, 712, 833
Conroy C., van Dokkum P., 2012a, ApJ, 747, 69
Conroy C., van Dokkum P., 2012b, ApJ, 760, 71
Conroy C., Wechsler R. H., 2009, ApJ, 696, 620
Conroy C., Gunn J. E., White M., 2009, ApJ, 699, 486
Conroy C., White M., Gunn J. E., 2010, ApJ, 708, 58
Crocker A. F., Bureau M., Young L. M., Combes F., 2011, MNRAS, 410, 1197
Crocker A. et al., 2012, MNRAS, 421, 1298
Croton D. J. et al., 2006, MNRAS, 365, 11
Da Rio N., Robberto M., Hillenbrand L. A., Henning T., Stassun K. G., 2012, ApJ, 748, 14
Daddi E. et al., 2010, ApJ, 713, 686
Dalgarno A., McCray R. A., 1972, ARA&A, 10, 375
Davé R., 2008, MNRAS, 385, 147
Davé R., Oppenheimer B. D., Finlator K., 2011, MNRAS, 415, 11
Davé R., Finlator K., Oppenheimer B. D., 2012, MNRAS, 421, 98
Davis T. A. et al., 2011, MNRAS, 417, 882
Dekel A. et al., 2009, Nat, 457, 451
Dib S., Bell E., Burkert A., 2006, ApJ, 638, 797
Downes D., Solomon P. M., 1998, ApJ, 507, 615
Draine B. T., 2011, in Draine B. T., ed., Physics of the Interstellar and Intergalactic Medium. Princeton Univ. Press, Princeton
Draine B. T., Li A., 2007, ApJ, 657, 810
Dutton A. A. et al., 2012, MNRAS, 428, 3183
Dwek E., 1998, ApJ, 501, 643
Elmegreen B. G., Klessen R. S., Wilson C. D., 2008, ApJ, 681, 365
Evans N. J., II, 1999, ARA&A, 37, 311
Fakhouri O., Ma C.-P., Boylan-Kolchin M., 2010, MNRAS, 406, 2267
Fardal M. A., Katz N., Weinberg D. H., Davé R., 2007, MNRAS, 379, 985
Faucher-Giguère C.-A., Kereš D., Ma C.-P., 2011, MNRAS, 417, 2982
Ferreras I., La Barbera F., de Carvalho R. R., de la Rosa I. G., Vazdekis A., Falcon-Barroso J., Ricciardelli E., 2012, MNRAS, 429, L15
Finlator K., Davé R., 2008, MNRAS, 385, 2181
Förster Schreiber N. M., Genzel R., Lutz D., Sternberg A., 2003, ApJ, 599, 193
Fukui Y., Kawamura A., 2010, ARA&A, 48, 547
Fumagalli M., da Silva R. L., Krumholz M. R., 2011, ApJ, 741, L26
Glover S. C. O., Mac Low M.-M., 2011, MNRAS, 412, 337
Gnedin N. Y., 2000, ApJ, 542, 535
Goldsmith P. F., 2001, ApJ, 557, 736
Groves B., Dopita M. A., Sutherland R. S., Kewley L. J., Fischera J., Leitherer C., Brandl B., van Breugel W., 2008, ApJS, 176, 438
Gunawardhana M. L. P. et al., 2011, MNRAS, 415, 1647
Hayward C. C., Narayanan D., Jonsson P., Cox T. J., Kereš D., Hopkins P. F., Hernquist L., 2010, in Treyer M., Lee J. C., Seibert M., Wyder, Neil J. D., eds, Conference Proceedings for UP2010: Have Observations Revealed a Variable Upper End of the Initial Mass Function? Astron. Soc. Pac., San Francisco, p. 369

Hayward C. C., Kereš D., Jonsson P., Narayanan D., Cox T. J., Hernquist L., 2011, ApJ, 743, 159
Hayward C. C., Jonsson P., Kereš D., Magnelli B., Hernquist L., Cox T. J., 2012a, MNRAS, 424, 951
Hayward C. C., Narayanan D., Kereš D., Jonsson P., Hopkins P. F., Cox T. J., Hernquist L., 2012b, MNRAS, 428, 2529
Hennebelle P., Chabrier G., 2008, ApJ, 684, 395
Hernquist L., 1990, ApJ, 356, 359
Hocuk S., Spaans M., 2010, A&A, 522, A24
Hocuk S., Spaans M., 2011, A&A, 536, A41
Holden B. P., van der Wel A., Kelson D. D., Franx M., Illingworth G. D., 2010, ApJ, 724, 714
Hopkins P. F., 2012, MNRAS, 423, 2037
Hopkins A. M., Beacom J. F., 2006, ApJ, 651, 142
Hopkins P. F., Richards G. T., Hernquist L., 2007, ApJ, 654, 731
Hopkins P. F., Younger J. D., Hayward C. C., Narayanan D., Hernquist L., 2010, MNRAS, 402, 1693
Ilbert O. et al., 2010, ApJ, 709, 644
Jeans J. H., 1902, R. Soc. Lond. Philos. Trans. Ser. A, 199, 1
Johnstone D., Fich M., Mitchell G. F., Moriarty-Schieven G., 2001, ApJ, 559, 307
Jonsson P., 2006, MNRAS, 372, 2
Jonsson P., Primack J. R., 2010, New Astron., 15, 509
Jonsson P., Cox T. J., Primack J. R., Somerville R. S., 2006, ApJ, 637, 255
Jonsson P., Groves B. A., Cox T. J., 2010, MNRAS, 403, 17
Joung M. R., Mac Low M., Bryan G. L., 2009, ApJ, 704, 137
Juneau S., Narayanan D. T., Moustakas J., Shirley Y. L., Bussmann R. S., Kennicutt R. C., Vanden Bout P. A., 2009, ApJ, 707, 1217
Kennicutt R. C., Jr, 1998b, ApJ, 498, 541
Kennicutt R. C., Jr, 1998a, ARA&A, 36, 189
Kennicutt R. C., Jr et al., 2003, PASP, 115, 928
Kennicutt R. C., Jr, Evans N. J., II, 2012, ARA&A, 50, 531
Kim D.-W. et al., 2009, ApJ, 703, 829
Klessen R. S., Spaans M., Jappsen A.-K., 2007, MNRAS, 374, L29
Kroupa P., 2002, Sci, 295, 82
Kroupa P., Tout C. A., Gilmore G., 1993, MNRAS, 262, 545
Kroupa P., Weidner C., Pflamm-Altenburg J., Thies I., Dabringhausen J., Marks M., Maschberger T., 2013, in Oswalt T. D., Gilmore G., eds, Planets, Stars and Stellar Systems, Vol. 5, Springer Science+Business Media, Dordrecht, p. 115
Krumholz M. R., 2011, ApJ, 743, 110
Krumholz M. R., Thompson T. A., 2007, ApJ, 669, 289
Krumholz M. R., McKee C. F., Tumlinson J., 2008, ApJ, 689, 865
Krumholz M. R., McKee C. F., Tumlinson J., 2009a, ApJ, 693, 216
Krumholz M. R., McKee C. F., Tumlinson J., 2009b, ApJ, 699, 850
Krumholz M. R., Leroy A. K., McKee C. F., 2011, ApJ, 731, 25
Krumholz M. R., Dekel A., McKee C. F., 2012, ApJ, 745, 69
Lada C. J., Lada E. A., 2003, ARA&A, 41, 57
Larson R. B., 1998, MNRAS, 301, 569
Larson R. B., 2005, MNRAS, 359, 211
Lee H., Bettens R. P. A., Herbst E., 1996, A&AS, 119, 111
Lee J. C. et al., 2009, ApJ, 706, 599
Leitherer C. et al., 1999, ApJS, 123, 3
Lemaster M. N., Stone J. M., 2008, ApJ, 682, L97
Luhman K. L., 2004, ApJ, 617, 1216
Luhman K. L., Briceño C., Stauffer J. R., Hartmann L., Barrado y Navascués D., Caldwell N., 2003, ApJ, 590, 348
Marchesini D., van Dokkum P. G., Förster Schreiber N. M., Franx M., Labbé I., Wuyts S., 2009, ApJ, 701, 1765
McDermid R. M. et al., 2012, in Tuffs R. J., Popescu C. C., eds, Proc. IAU Symp. 284, The Spectral Energy Distribution of Galaxies. Cambridge Univ. Press, Cambridge, p. 244
McKee C. F., Ostriker J. P., 1977, ApJ, 218, 148
McKee C. F., Ostriker E. C., 2007, ARA&A, 45, 565
Meurer G. R. et al., 2009, ApJ, 695, 765
Miller G. E., Scalo J. M., 1979, ApJS, 41, 513
Mo H. J., Mao S., White S. D. M., 1998, MNRAS, 295, 319
Moster B. P., Macciò A. V., Somerville R. S., Naab T., Cox T. J., 2011, MNRAS, 415, 3750
Moster B. P., Maccio' A. V., Somerville R. S., Naab T., Cox T. J., 2012, MNRAS, 423, 2045
Motte F., André P., Ward-Thompson D., Bontemps S., 2001, A&A, 372, L41
Narayanan D., Davé R., 2012, MNRAS, 423, 3601
Narayanan D., Cox T. J., Hernquist L., 2008a, ApJ, 681, L77
Narayanan D., Cox T. J., Shirley Y., Davé R., Hernquist L., Walker C. K., 2008b, ApJ, 684, 996
Narayanan D., Hayward C. C., Cox T. J., Hernquist L., Jonsson P., Younger J. D., Groves B., 2010a, MNRAS, 401, 1613
Narayanan D. et al., 2010b, MNRAS, 407, 1701
Narayanan D., Cox T. J., Hayward C. C., Hernquist L., 2011a, MNRAS, 412, 287
Narayanan D., Krumholz M., Ostriker E. C., Hernquist L., 2011b, MNRAS, 418, 664
Narayanan D., Krumholz M. R., Ostriker E. C., Hernquist L., 2012a, MNRAS, 421, 3127
Narayanan D., Bothwell M., Davé R., 2012b, MNRAS, 426, 1178
Nayakshin S., Sunyaev R., 2005, MNRAS, 364, L23
Noeske K. G. et al., 2007a, ApJ, 660, L47
Noeske K. G. et al., 2007b, ApJ, 660, L43
Nutter D., Ward-Thompson D., 2007, MNRAS, 374, 1413
Okamoto T., Gao L., Theuns T., 2008, MNRAS, 390, 920
Oppenheimer B. D., Davé R., Kereš D., Fardal M., Katz N., Kollmeier J. A., Weinberg D. H., 2010, MNRAS, 406, 2325
Ostriker E. C., Shetty R., 2011, ApJ, 731, 41
Ostriker E. C., Stone J. M., Gammie C. F., 2001, ApJ, 546, 980
Ostriker E. C., McKee C. F., Leroy A. K., 2010, ApJ, 721, 975
Pacifici C., Kassin S. A., Weiner B., Charlot S., Gardner J. P., 2012, ApJ, 762, L15
Padoan P., Nordlund Å., 2002, ApJ, 576, 870
Papadopoulos P. P., 2010, ApJ, 720, 226
Papadopoulos P. P., Thi W.-F., Miniati F., Viti S., 2011, MNRAS, 414, 1705
Pérez-González P. G. et al., 2008, ApJ, 675, 234
Rayner J. T., Cushing M. C., Vacca W. D., 2009, ApJS, 185, 289
Reddy N. A., Steidel C. C., 2009, ApJ, 692, 778
Rieke G. H., Loken K., Rieke M. J., Tamblyn P., 1993, ApJ, 412, 99
Robertson B., Yoshida N., Springel V., Hernquist L., 2004, ApJ, 606, 32
Robertson B., Hernquist L., Cox T. J., Di Matteo T., Hopkins P. F., Martini P., Springel V., 2006, ApJ, 641, 90
Robitaille T. P., Whitney B. A., 2010, ApJ, 710, L11
Rodighiero G. et al., 2011, ApJ, 739, L40
Sakamoto K., Scoville N. Z., Yun M. S., Crosas M., Genzel R., Tacconi L. J., 1999, ApJ, 514, 68
Salpeter E. E., 1955, ApJ, 121, 161
Satyapal S., Watson D. M., Pipher J. L., Forrest W. J., Greenhouse M. A., Smith H. A., Fischer J., Woodward C. E., 1997, ApJ, 483, 148
Schmidt M., 1959, ApJ, 129, 243
Schöier F. L., van der Tak F. F. S., van Dishoeck E. F., Black J. H., 2005, A&A, 432, 369
Silk J., 1995, ApJ, 438, L41
Smith R. J., Lucey J. R., Carter D., 2012, MNRAS, 426, 2994
Sobral D., Best P. N., Matsuda Y., Smail I., Geach J. E., Cirasuolo M., 2012, MNRAS, 420, 1926
Spiniello C., Koopmans L. V. E., Trager S. C., Czoske O., Treu T., 2011, MNRAS, 417, 3000
Spiniello C., Trager S. C., Koopmans L. V. E., Chen Y. P., 2012, ApJ, 753, L32
Springel V., 2005, MNRAS, 364, 1105
Springel V., Hernquist L., 2003, MNRAS, 339, 289
Springel V., Di Matteo T., Hernquist L., 2005, MNRAS, 361, 776
Stark D. P., Schenker M. A., Ellis R. S., Robertson B., McLure R., Dunlop J., 2012, ApJ, 763, 129
Stolte A., Brandner W., Grebel E. K., Lenzen R., Lagrange A.-M., 2005, ApJ, 628, L113

Tacconi L. J. et al., 2008, ApJ, 680, 246
Tacconi L. J. et al., 2010, Nat, 463, 781
Thomas D., Maraston C., Bender R., Mendes de Oliveira C., 2005, ApJ, 621, 673
Tortora C., Romanowsky A. J., Napolitano N. R., 2012, ApJ, 765, 8
Trager S. C., Faber S. M., Worthey G., González J. J., 2000, AJ, 119, 1645
Trager S. C., Faber S. M., Dressler A., 2008, MNRAS, 386, 715
Treu T., Auger M. W., Koopmans L. V. E., Gavazzi R., Marshall P. J., Bolton A. S., 2010, ApJ, 709, 1195
Tumlinson J., 2007, ApJ, 664, L63
van de Sande J. et al., 2011, ApJ, 736, L9
van Dokkum P. G., 2008, ApJ, 674, 29
van Dokkum P. G., Conroy C., 2010, Nat, 468, 940
van Dokkum P., Conroy C., 2012, ApJ, 760, 70
Vázquez G. A., Leitherer C., 2005, ApJ, 621, 695
Vladilo G., 1998, ApJ, 493, 583
Wake D. A. et al., 2011, ApJ, 728, 46
Weidner C., Kroupa P., Pflamm-Altenburg J., 2011, MNRAS, 412, 979
Weidner C., Ferreras I., Vazdekis A., La Barbera F., 2013, MNRAS, 435, 2274
Weingartner J. C., Draine B. T., 2001, ApJ, 548, 296
Weisz D. R. et al., 2012, ApJ, 744, 44
Wilkins S. M., Trentham N., Hopkins A. M., 2008, MNRAS, 385, 687
Wing R. F., Ford W. K., Jr, 1969, PASP, 81, 527
Wolfire M. G., Hollenbach D., McKee C. F., 2010, ApJ, 716, 1191
Xu X., Narayanan D., Walker C., 2010, ApJ, 721, L112
Young L. M. et al., 2011, MNRAS, 414, 940
Zaritsky D., Colucci J. E., Pessev P. M., Bernstein R. A., Chandar R., 2013, ApJ, 770, 121

This paper has been typeset from a TEX/LATEX file prepared by the author.